

Dagmar Flöck  
Isabella Daidone  
Alfredo Di Nola  
Department of Chemistry,  
University of Rome "La  
Sapienza," P.le Aldo Moro 5,  
Rome 00185, Italy

# A Molecular Dynamics Study of Acylphosphatase in Aggregation-Promoting Conditions: The Influence of Trifluoroethanol/Water Solvent

Received 20 July 2004;  
accepted 2 September 2004  
Published online 3 November 2004 in Wiley InterScience (www.interscience.wiley.com). DOI 10.1002/bip.20166

**Abstract:** The 98-residue protein acylphosphatase exhibits a high propensity for aggregation under certain conditions. Aggregates formed from wild-type acylphosphatase in the presence of 2,2,2-trifluoroethanol and from highly destabilized mutants are essentially identical in structure. Furthermore, it has been shown by mutational studies that different regions of the protein are important for aggregation and folding. In the present molecular dynamics study, we compare the behavior of the protein in aqueous solution and in a 25 % (v/v) 2,2,2-trifluoroethanol/water environment mimicking the experimental conditions. The 2,2,2-trifluoroethanol surrounding affects the structure of the protein mostly in the regions important for aggregation, in good agreement with experimental data. This suggests that the early step of (partly) unfolding, which precedes the aggregation process, has been observed. © 2004 Wiley Periodicals, Inc. *Biopolymers* 75: 491–496, 2004

**Keywords:** protein aggregation; protein misfolding; essential dynamics

## INTRODUCTION

Acylphosphatase (AcP) is an  $\alpha/\beta$  protein (Figure 1) with five  $\beta$ -strands ( $\beta$  1: residues 7–13;  $\beta$  2: residues 36–42;  $\beta$  3: residues 46–53;  $\beta$  5: residues 93–97) and two  $\alpha$ -helices ( $\alpha$  1: residues 22–33;  $\alpha$  2: residues 55–65). The single-domain 98-amino-acid-residue protein catalyzes the hydrolysis of the carboxyl phosphate bond present in physiologically important molecules.<sup>1,2</sup> Recent investigations on the role of AcP in the ion transport mechanism have shown that it considerably affects the capacitive current transients that are directly related to the ion transport by  $\text{Na}^+$ ,  $\text{K}^+$ -ATPase.<sup>3</sup>

AcP has been shown to aggregate under appropriate conditions. Aggregation leads to the formation of the same type of highly organized amyloid fibrils associated with protein deposition diseases.<sup>4–6</sup> A detailed study of point mutations<sup>6</sup> indicated that different sections of the protein are responsible for the aggregation process on one side and for the folding process on the other side. In particular, it was shown that mutations that significantly disturb the rate of aggregation are located in two regions of the protein sequence, residues 16–31, corresponding to  $\alpha$ -helix 1 (see Figure 1) and the preceding loop, and residues 87–98, corresponding to the C-terminal region includ-

Correspondence to: Alfredo Di Nola; email: dinola@degas.chem.uniroma1.it

Contract grant sponsor: European Community Training and Mobility Research Network Project "Protein (Mis) folding"

Contract grant number: HPRN-CT-2002-00241

*Biopolymers*, Vol. 75, 491–496 (2004)

© 2004 Wiley Periodicals, Inc.

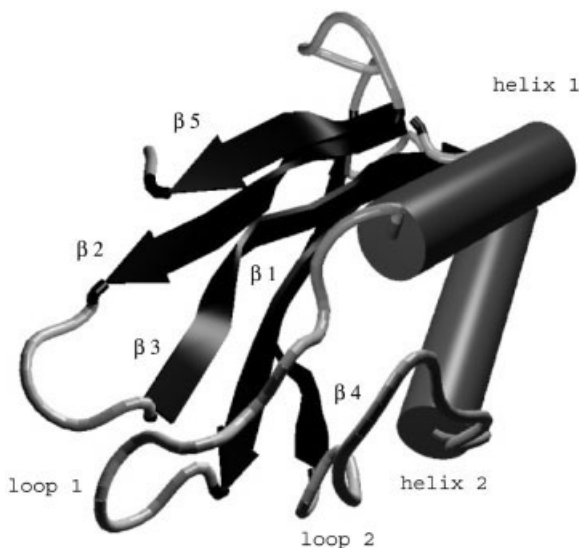


**FIGURE 1** Cartoon representation of the three-dimensional structure of horse muscle acylphosphatase.<sup>11</sup> Elements of secondary structure are labeled.

ing a small  $\beta$ -sheet. Both regions showed high  $\beta$ -sheet propensity. The experimental results suggested that they could be responsible for initiating the process of aggregation. These studies were performed in aqueous solutions containing 25% 2,2,2-trifluoroethanol (TFE), which unfolds the protein but still allows aggregation to occur.<sup>4,5</sup> The insights gained by these systematic experimental studies make AcP an ideal model system for computational studies of the early stage of protein aggregation.

Here, we present a molecular dynamics (MD) study of AcP that investigates the effect of TFE, in comparison with a simple aqueous solution, on the protein. Additional to the standard MD analysis, an essential dynamics (ED) analysis<sup>7,8</sup> is performed to investigate the principal features of motion.

## METHODS

### MD Simulations

The 98-residue protein AcP was investigated in a 25% (v/v) TFE/water mixture and a pure aqueous solution for comparison. All simulations were performed and analyzed with the GROMACS software package and the GROMOS96 force field.<sup>9,10</sup> The starting configuration was taken from the first NMR structure of horse muscle AcP, Protein Data Bank (PDB) entry code 1APS.<sup>11</sup> The pH of 5.5 was realized by the setting of the protonation states of the ionizable residues according to their  $pK_a$ 's. The protein was in one case immersed in a rectangular box ( $x = 6.00$  nm,  $y = 5.66$  nm,  $z = 4.90$  nm) of Single Point Charge (SPC) water molecules,<sup>12</sup> in the other in a rectangular box of same size with

a 25% TFE molecule content. The TFE/SPC model was taken from Fioroni et al.<sup>13,14</sup> In order to increase the time step to 4 fs, hydrogen atoms were simulated as dummy atoms.<sup>15</sup> To slow down the high-frequency motions of the water and TFE molecules, the mass of water hydrogens and of the hydroxyl hydrogen of TFE were increased from 1u to 4u, while the mass of the oxygen was reduced in order to maintain the total molecule mass.<sup>15</sup> To achieve charge neutrality of the system, six chloride counterions were inserted to substitute water molecules in positions where the electrostatic potential was most favorable. Simulations were performed in the canonical (NVT) ensemble, with temperatures kept close to the desired value (298 K) by a weak coupling to an external heat bath.<sup>16</sup> The coupling constant was chosen to match the time step. The LINCS algorithm was used to constrain bond lengths.<sup>17</sup> Long-range electrostatic interactions were calculated using the particle-mesh Ewald (PME) method.<sup>18</sup> For the PME calculation the spacing of the Fourier-transformed grid was set to 0.12 nm and the relative strength of the electrostatic interaction at the cutoff to  $1e-05$ . The cutoff radius for the Lenard-Jones interactions was set to 0.9 nm.

After a subsequent energy minimization of solvent and protein and a 100-ps relaxation of the solvent, the system temperature was gradually increased from 50 K to 298 K over 100 ps. The production runs were performed for 80 ns each.

Although the length of the simulations furnishes enough statistics, additional simulations at  $T = 323$  K for 45 ns were performed both in water and in TFE/water mixtures. The results were almost indistinguishable from the simulation at  $T = 298$  K. In the results section, only the results obtained at 298 K will be reported.

### ED Analysis

Standard ED analysis<sup>7,8</sup> was performed on the equilibrated portion of the AcP trajectory in aqueous solution (5–80 ns). A covariance matrix of the  $C_\alpha$  atoms positional fluctuations was built. Its diagonalizing yielded the principal directions of large-amplitude fluctuations of the protein. In the case of the unfolding dynamics of AcP in the 25% (v/v) TFE/water mixture, we are more interested in the deviations from a reference structure rather than in the equilibrium fluctuations. Hence a variation of ED analysis<sup>19</sup> was used, which calculates the deviations with respect to the starting reference structure, which is the minimized NMR structure rather than fluctuations around the average conformation, as in the standard procedure. The analysis was performed on the first 15 ns of the trajectory, so that the internal motions that deform the protein structure were taken into account.

## RESULTS AND DISCUSSION

The MD simulation of AcP in aqueous solution at room temperature showed an overall stability of the

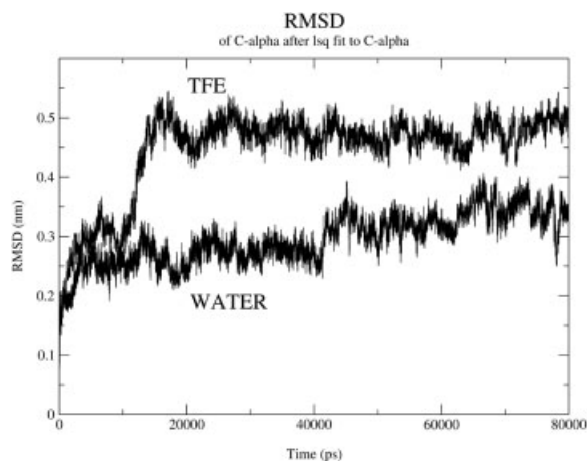


**FIGURE 2** RMSD of  $C_{\alpha}$  positions compared to the minimized NMR structure for the simulation in aqueous simulation and TFE/water mixture.

root mean square deviation (RMSD) of  $C_{\alpha}$  positions compared to the minimized NMR structure (see Figure 2). The secondary structure elements of the NMR structure showed little distortion throughout the 80-ns simulation (data not shown) with the exception of the small  $\beta$ -sheet ( $\beta 5$ ) at the C-terminal (residues 94–98), which transformed to a mere  $\beta$ -bend. The dynamic properties of the simulation were determined by performing essential dynamics analysis on the  $C_{\alpha}$  atoms. The highest atom displacements along the first eigenvectors were observed in the loop region connecting  $\beta 1$  and  $\alpha 1$  (loop 1), the bend between  $\beta 2$  and  $\beta 3$  and another loop region connecting  $\alpha 2$  and  $\beta 4$  (loop 2). These three regions are located in close proximity to each other and include part of the active site.<sup>20</sup>

In contrast, the simulation of AcP in TFE exhibits the instability of the native fold in this environment. The RMSD of  $C_{\alpha}$  reaches a value of 0.5 nm within the first 15 ns and undergoes small fluctuations during the rest of the simulation (see Figure 2). Also in this environment, the secondary structure elements are quite undisturbed throughout the simulation time. The tertiary structure, on the other hand, is only stable for the first 10 ns. In the following, the most striking dynamic feature of the simulation occurs: the  $\alpha$ -helix 1 tilts outwardly for almost  $50^{\circ}$  and opens the native fold of the protein (see Figure 3). We have performed a principal component analysis of the deformation of the protein in the first 15 ns in TFE (see methods section). The average structure of the simulation in pure water was chosen as reference. Figure 4 shows the average  $C_{\alpha}$  displacement along the first eigenvector (with the largest eigenvalue). It can be noted that the dynamics consists mainly of the coupled movements of residues 17–29 (loop 1 and almost all of

helix 1) and residues 64–72 (last part of helix 2 and loop 2). The first of the above-mentioned regions corresponds exactly to one of the regions that have been shown to be most important for aggregation.<sup>6</sup> The loop region including residues 68–72 (loop 2) is located in close proximity to the  $\alpha$ -helix and the loop preceding it, which explains the dynamical coupling between these regions. Also, part of the C-terminal region (residues 96 and 97), which was found important for aggregation, shows a large deviation with respect to the rest of the protein. In a previously reported unfolding simulation<sup>19</sup> of cytochrome *c*, we showed that unfolding occurred along one of the principal fluctuation eigenvectors of the native protein. In the present case, the analogous analysis shows that the motions of deformation are not represented in the first ten eigenvectors of the simulation in water. This indicates that a new direction of motion is activated in TFE.

The interresidue side-chain contact map (with a minimum distance of 6 Å between any two atoms) showed that on average 1.5 contacts are lost per residue after the 80-ns simulation in TFE compared to the average protein structure in water. The region of



**FIGURE 3** Cartoon representation of AcP structure. Comparison between the NMR structure (black)<sup>11</sup> and the structure after a 80 ns simulation in 25% TFE/water mixture (gray).

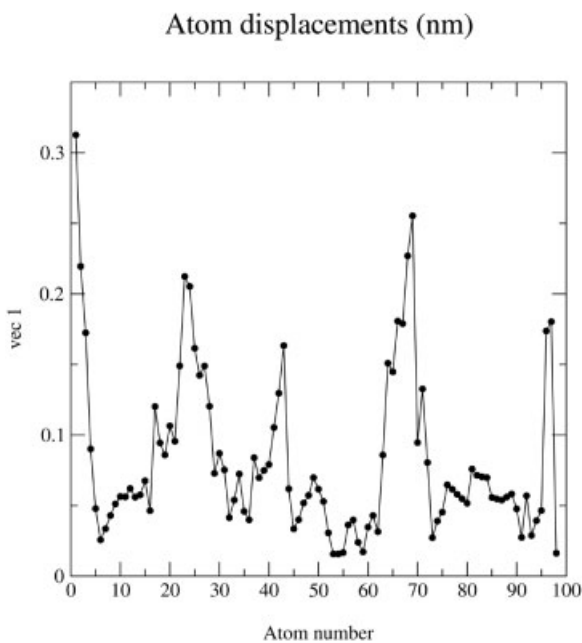


**FIGURE 4** Atom displacement along the first eigenvector of principal components analysis in reference to the average structure of the simulation in aqueous solution. High values indicate the motions of deformation caused by the TFE environment.

the protein exhibiting the highest loss is helix 1, with an average value of 2.4 contacts lost per residue. It should be pointed out that the secondary structure of

the  $\alpha 1$  helical region is well conserved (see Figure 3); hence, it can be concluded that in TFE the motion of this region is mainly a rigid motion leading to the disruption of its tertiary structure.

It is interesting to investigate the special interactions of TFE molecules with different residues. Our analysis shows that TFE builds dense hydrogen-bonding networks with the charged residues of the protein while water molecules cannot be found in the immediate neighborhood. Two exemplary snapshots of intermolecular interactions formed with negatively charged and positively charged side chains are shown in Figure 5 and Figure 6, respectively. TFE also clusters around hydrophobic side chains with its trifluoride head. Indeed, it has been shown recently<sup>21</sup> that the TFE interaction with hydrophobic groups in the amino acids dominates over the interaction of the ionic and hydrophilic groups of the amino acids with the carboxyl group of the alcohol.

The same article reports that it is the decreased surface tension of water in the presence of TFE that leads to a preferential exclusion of water molecules from the protein and to a destabilization (of the tertiary structure) of the protein by disrupting the interaction that the protein had with the surrounding water. On the other hand, the low dielectric environment and the removal of alternative hydrogen-bonding partners favors the formation of intrapeptide hydrogen

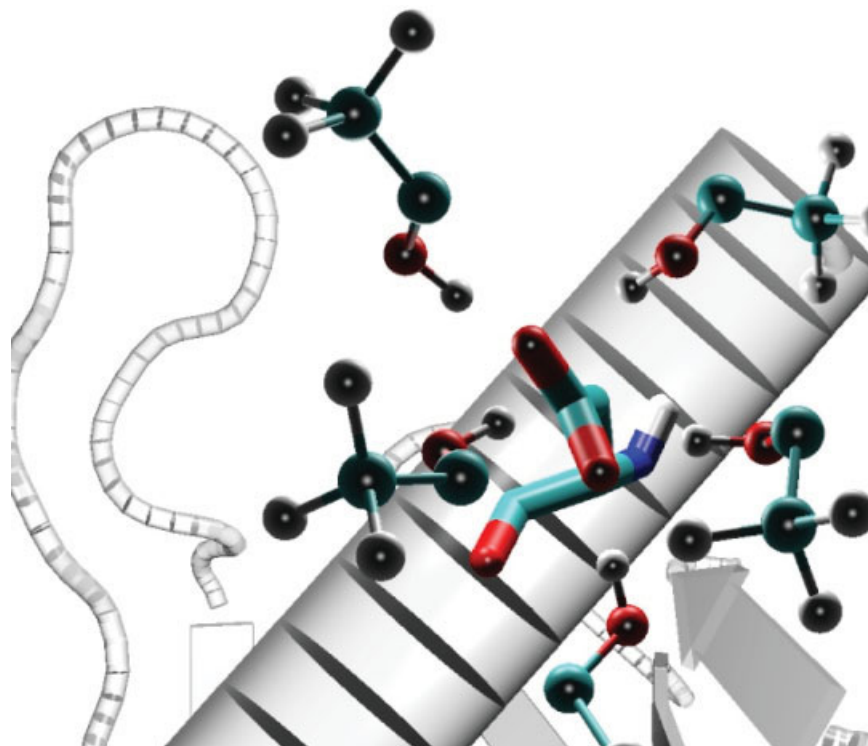


**FIGURE 5** Hydrogen-bonding network between Asp 28 and surrounding TFE molecules.

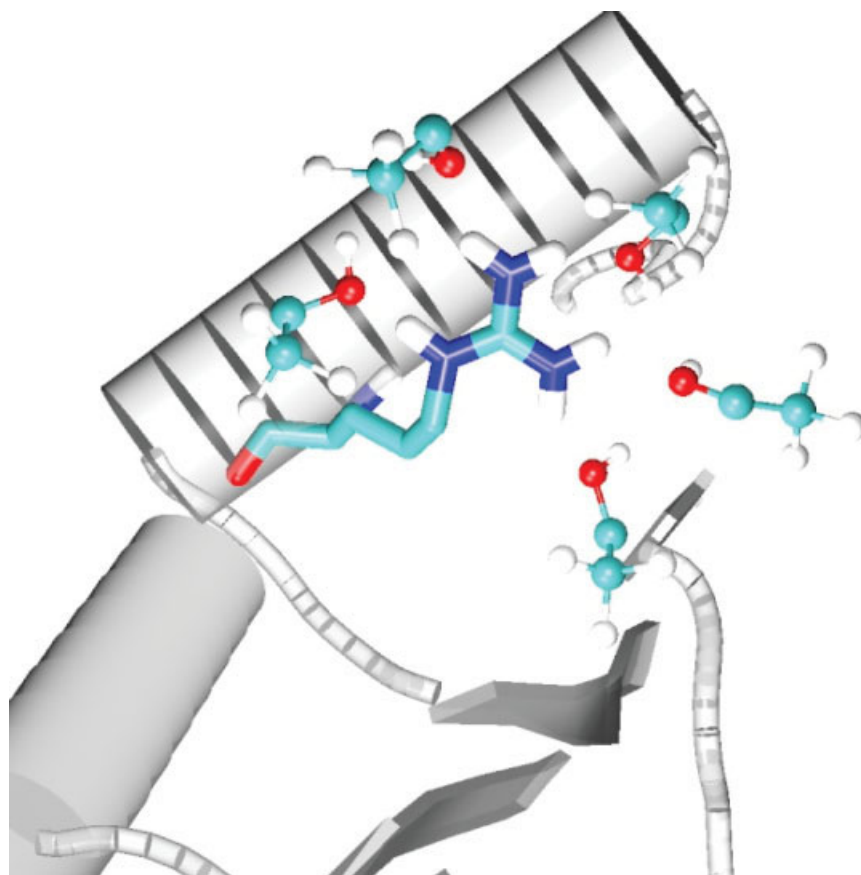


**FIGURE 6** Hydrogen-bonding network between Arg 31 and surrounding TFE molecules.

bonds.<sup>14,22</sup> The disruption of the tertiary structure of AcP in the reported TFE/water mixture and maintenance of secondary structure elements that we observe in our MD study are in excellent agreement with both findings.

As already mentioned above, helix 1 loses almost all contacts with the surrounding secondary structure elements. A closer look at the side-chain contacts within the helix reveals that multiple intramolecular salt bridges that stabilize the helix (E27–R31, D28–R31, D28–K32, E29–K32) are maintained during the TFE simulation. We speculate that these salt bridges are not disrupted because secondary structures maintaining H-bonds are stabilized (as discussed above) and the side chains optimize their interaction.

Furthermore, there might be a second argument why TFE affects the two helices of the protein differently. According to the hydrophathy scale of Kyte and Doolittle,<sup>23</sup> helix 2 is much less hydrophobic than helix 1. While for helix 1 the averaged hydrophathy value per residue is  $-0.64$ , it is  $-1.20$  for helix 2. Since TFE reduces the hydrophobic effect in water,<sup>24</sup> this difference in hydrophathy might be able to explain why helix 2 is hardly affected by the TFE environ-

ment while helix 1 loses most of its interresidue contacts with the  $\beta$ -sheet and the other helix, and performs a rigid body movement that opens the tertiary structure of the protein.

## CONCLUSION

Although the time range of the performed MD simulations does not allow us to speculate on the details of the aggregation process, it is interesting to observe that the present results are in good agreement with the experimental data.<sup>6</sup> The data presented here suggest that the movement of  $\alpha$ -helix 1 initiates the (partly) unfolding of the protein that precedes the aggregation process.

It is known that TFE, apart from reducing the hydrophobic effect in water, is able to stabilize individual secondary structure elements by stabilizing the peptide hydrogen bond.<sup>24</sup> It is also known that addition of TFE to the solution surrounding a protein can accelerate the aggregation process.<sup>4,5</sup> Therefore, the unfolding dynamics suggested here that precedes the aggregation process is in good agreement with both

findings. The coating of the protein with TFE displaces the usual water coating and has different effects on peptide hydrogen bonding (strengthening) and hydrophobic interactions between secondary structure elements (weakening).

It seems that TFE enhances aggregation by promoting the rigid body movement of helix 1. Interestingly, helix 1 has a very high  $\beta$ -sheet propensity.<sup>6</sup> Later on in the aggregation process it will most probably unfold and then refold as a  $\beta$ -sheet. This process might be greatly facilitated by the opening of the tertiary structure that we observed here.

We thank Dr. Danilo Roccatano for valuable discussions. This work was supported by the European Community Training and Mobility Research Network Project "Protein (mis) Folding": HPRN-CT-2002-00241.

## REFERENCES

- Ramponi, G.; Melani, F.; Guerritore, A. G *Biochim* 1961, 10, 189–196.
- Stefani, M.; Taddei, N.; Ramponi, G. *Cell Mol Life Sci* 1997, 53, 141–151.
- Tadini-Buoninsegni, F.; Nassi, P.; Nediani, C.; Dolfi, A.; Guidelli, R. *Biochem Biophys Acta* 2003, 1611, 70–80.
- Chiti, F.; Webster, P.; Taddei, N.; Clark, A.; Stefani, M.; Ramponi, G.; Dobson, C. M. *Proc Natl Acad Sci* 1999, 96, 3590–3594.
- Chiti, F.; Taddei, N.; Bucciantini, M.; White, P.; Ramponi, G.; Dobson, C. M. *EMBO J* 2000, 19, 1441–1449.
- Chiti, F.; Taddei, N.; Baroni, F.; Capanni, C.; Stefani, M.; Ramponi, G.; Dobson, C. M. *Nat Struct Biol* 2002, 9, 137–143.
- Amadei, A.; Linssen, A. B. M.; Berendsen, H. J. C. *Proteins Struct Funct Genet* 1993, 17, 412–425.
- de Groot, B. L.; Amadei, A.; Scheek, R. M.; van Nuland, N. A.; Berendsen, H. J. C. *Proteins Struct Funct Genet* 1996, 26, 314–322.
- van der Spoel, D.; van Drunen, R.; Berendsen, H. J. C. *GRONINGEN MACHINE for Chemical Simulation*. Department of Biophysical Chemistry, BIOSON Research Institute, Nijenborgh 4 NL-9717 AG Groningen, 1994. e-mail to gromacs@chem.rug.nl.
- van Gunsteren, W. F.; Billeter, S.; Eising, A.; Hünenberger, P.; Kruger, P.; Mark, A. E.; Scott, W.; Tironi, I. *Biomolecular Simulations: The GROMOS96 Manual and User Guide*. Zürich; Groningen: Biomos b.v., 1996.
- Pastore, A.; Saudek, V.; Ramponi, G.; Williams, R. J. *J Mol Biol* 1992, 224, 427–440.
- Berendsen, H. J. C.; Postma, J. P. M.; van Gunsteren, W. F.; Hermans, J. In *Intermolecular Forces*; Pullman, B., Ed.; D. Reidel Publishing Company: Dordrecht, The Netherlands, 1981; pp 331–342.
- Fioroni, M.; Burger, K.; Mark, A. E.; Roccatano, D. *J Phys Chem B* 2000, 104, 12347–12354.
- Roccatano, D.; Colombo, G.; Fioroni, M.; Mark, A. E. *Proc Natl Acad Sci USA* 2002, 99, 12179–12184.
- Feenstra, K. A.; Hess, B.; Berendsen, H. J. C. *J Comp Chem* 1999, 20, 786–798.
- Berendsen, H. J. C.; Postma, J. P. M.; van Gunsteren, W. F.; Di Nola, A.; Haak, J. R. *J Chem Phys* 1984, 81, 3684–3690.
- Hess, B.; Bekker, H.; Berendsen, H. J. C.; Fraaije, J. G. E. M. *J Comp Chem* 1997, 18, 1463–1472.
- Darden, T.; York, D.; Pedersen, L. *J Chem Phys* 1993, 98, 10089–10092.
- Roccatano, D.; Daidone, I.; Ceruso, M.-A.; Bossa, C.; Di Nola, A. *Biophys J* 2003, 84, 1876–1883.
- Taddei, N.; Stefani, M.; Magherini, F.; Chiti, F.; Modesti, A.; Raugei, G.; Ramponi, G. *Biochemistry* 1996, 35, 7077–1083.
- Kundu, A.; Kishore, N. *Biophys Chem* 2004, 109, 427.
- Luo, P.; Baldwin, R. L. *Biochemistry* 1997, 36, 8413.
- Kyte, J.; Doolittle, R. F. *J Mol Biol* 1982, 157, 105–132.
- Luo, P.; Baldwin, R. L. *Proc Natl Acad Sci* 1999, 96, 4930–4935.

*Reviewing Editor: Andrew J. McCammon*